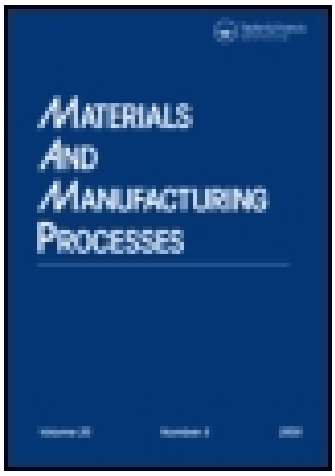

Materials and Manufacturing Processes
Publication details, including instructions for authors and subscription information:
http://www.tandfonline.com/loi/lmmp20

Laser Spot Welding of Thermoplastic and Ceramic: An Experimental Investigation

K. F. Tamrin[ab], Y. Nukman[a] & N. A. Sheikh[c]

[a] Department of Mechanical Engineering, Faculty of Engineering, University of Malaya, Kuala Lumpur, Malaysia

[b] Computing Department, Faculty of Arts, Computing and Creative Industry, Sultan Idris Education University (UPSI), Tanjong Malim, Perak, Malaysia

[c] Department of Mechanical Engineering, Mohammad Ali Jinnah University, Islamabad, Pakistan

Accepted author version posted online: 09 Mar 2015.Published online: 09 Mar 2015.

Materials and Manufacturing Processes, 0: 1–8, 2015

ISSN: 1042-6914 print/1532-2475 online
DOI: 10.1080/10426914.2015.1019108

Taylor & Francis
Taylor & Francis Group

Laser Spot Welding of Thermoplastic and Ceramic: An Experimental Investigation

K. F. Tamrin[1,2], Y. Nukman[1], and N. A. Sheikh[3]

[1]*Department of Mechanical Engineering, Faculty of Engineering, University of Malaya, Kuala Lumpur, Malaysia*
[2]*Computing Department, Faculty of Arts, Computing and Creative Industry, Sultan Idris Education University (UPSI), Tanjong Malim, Perak, Malaysia*
[3]*Department of Mechanical Engineering, Mohammad Ali Jinnah University, Islamabad, Pakistan*

Laser welding of dissimilar materials classes has vast potential in a variety of applications due to the non-contact nature of the process. This study investigates the effects of CO_2 laser process parameters on the characteristics of spot welded joint between ceramic and thermoplastic. Using a full-factorial design an experimental investigation is carried out studying the effect of welding parameters (laser exposure, number of spots, stand-off distance) on the tensile strength and the diameter of spot weld. The study reveals an increase of joint tensile strength with the increase in the number of spots and the duration of exposure. However at low laser power, the effect of stand-off distance on the spot weld diameter is found to be inconclusive. Optimal process parameters are estimated using the multi-objective optimization on the basis of ratio analysis. The analysis shows that the higher number of spots and the longest duration of laser exposure result in optimal weld characteristics. Alongside these conditions, a larger stand-off distance is seen to have beneficial impact on the weld characteristics.

Keywords Ceramic; Dissimilar; Joining; Laser; Optimization; Spot; Thermoplastic; Welding.

Introduction

Laser processing of dissimilar materials has gained attention in recent years. With increase in the use of low cost non-conventional materials in areas of aerospace, automotive, micro-electro-mechanical systems (MEMS), petrochemical, nuclear, and electronics industries; the use of laser processing is of greater benefit compared to other techniques [1]. It offers adaptability, precise control, and greater accessibility compared to other conventional techniques. For instance a single laser source, depending on the power and speed, can be used for cutting as well as welding processing. The welding process can be controlled to either form a continuous bead or a more precise spot weld joint.

Laser processing is sustenance of future market demand for low weight, smart, and hybrid structures. However use of laser power for non-conventional materials is somewhat new. Only recently characteristic behavior of materials subjected to laser heating has been studied [2–5]. A comprehensive review by Tamrin et al. [6] summarizes the factors affecting the welding process of dissimilar material classes. Tamrin et al. highlighted the fact that laser welding is a complicated process involving a number of parameters such as laser intensity, traverse speed, and stand-off distance in addition to the characteristics/properties of the welding materials. In the case of a typical lap joint, it requires a transmissive top material so that the bottom material can absorb heat for local melting suggesting that the selection of optimum laser parameters is dependent on the welding material properties. The varsity of the process makes the use of laser welding for dissimilar material classes difficult and therefore is topic of research.

Laser welding of polymer and ceramics has numerous applications in the areas of biochemistry, bioreactor, micro-fluidics, micro-electronic sensors, micro-actuators, and lab-on-a-chip systems. For instance, the use of transparent polymer windows has been useful in the study of cellular growth inside biochemical and microbiological reactors using optical photometry and fluorescence measurements [7, 8]. In addition ceramic-polymer sensor systems have also been used for cell culture measurements. Therefore understanding, controlling, and optimization of laser welding of ceramics and polymers can be of greater benefit to medical technology, chemical, automobile, telecom, pharmaceutical, and food industries.

For polymer and ceramic welding, only few studies can be found despite their enormous benefits and applications. In one of the important studies Kawahito et al. [4] used diode laser ($\lambda = 940$ nm) for welding Si_3N_4 and PET. Using a 170 W laser power source with scanning speed of 4 mm/s, optimum bond strength of 3100 N was achieved in the absence of shielding gas. It was observed that the joint was bonded on the atomic level through an anchor effect along with bubble formation. The suggested mechanism for such weld morphology was linked to the flow of plastic, upon liquefaction, in

Received October 10, 2014; Accepted January 12, 2015

Address correspondence to K. F. Tamrin, Department of Mechanical Engineering, Faculty of Engineering, University of Malaya, 50603 Kuala Lumpur, Malaysia; E-mail: k.f.tamrin@outlook.com

Color versions of one or more of the figures in the article can be found online at www.tandfonline.com/lmmp.

to nano-scale pores of the ceramic [4]. Upon subsequent solidification, the atomic scale joint formation is observed. Recently Tamrin et al. [9] used grey relational analysis (GRA) to experimentally study properties of lap joint between polymer and ceramic with laser. Based on the three important observable parameters (joint strength, weld, and kerf width) optimal configuration of laser source parameters were estimated.

While for the laser spot welding only a handful of studies can be found in the literature. In comparison to other established contact based spot welding techniques (such as friction stir spot welding, resistance spot welding, fusion welding, ultrasonic welding etc.), laser spot welding is a non-contact process with minimum heat-affected zone (HAZ) [10, 11]. As in the case of non-intrusive electron beam welding, laser spot welding does not require vacuum environment to efficiently operate. However studies on laser spot welding of dissimilar materials are even more limited. Metal-plastic spot joints have been studied by Yusof et al. [12]. Yusof et al. observed that the joint strength is proportional to the molten pool depth. Although laser based technique called LIFTEC (laser-induced fusion technology) has been successfully used for welding metals and/or ceramics with polymers components and is foreseen to be used in automobile industry [13]. However the technique uses a transmitted laser beam through transparent plastic base to heat up metal/ceramic fastener. Due to localized heating, the plastic at the interface melts down. At this stage the fastener is pushed in to the melted block of plastic which forms a joint upon solidification. LIFTEC has limited applications for delicate materials and interfaces especially in the areas of bioMEMS.

The aim of this research is to study the important parameters involved in the laser spot welding process of dissimilar materials classes. Using a full-factorial experimental design three influential parameters is studied. By controlled variation of laser source stand-off distance, exposure duration of heat source and the number of spots; strength of the welded joint and its diameter are analyzed. All experiments are carried out using a CO_2 laser source for spot welding thermoplastic and ceramic substrates. Although the CO_2 laser interacts well with both the thermoplastic and ceramic substrates, however controlling the process is quite a challenge as both materials are susceptible to decomposition upon interaction with the laser. For optimizing multi-performance characteristics, GRA has also been employed by two disparate studies [9, 14]. Compared to GRA, MOORA offers a mathematically simple, straightforward, and easily applicable procedure for optimization problems. It can be applied to different manufacturing operations and scenarios as recently shown by Gadakh et al. [15] for welding processes including submerged arc, gas tungsten arc, gas metal arc, CO_2 laser, and friction stir welding. Here for the first time results are reported for laser spot welding of dissimilar welding class using MOORA.

The organization of the paper is as follows. Initially the detailed design of experiments is included along with the specification of laser facility and materials used. Next section includes the results and discussion on the effect of process parameters on weld tensile strength and weld diameter. Following the discussion, optimal performance parameters are presented for laser spot welding using MOORA method.

Materials and methods

For this experimental study thermoplastic PETG is used for laser spot welding with Macor glass ceramic [16]. PETG is often used in BioMEMS applications as it offers resistance to high moisture, oxygen, solvents, and degreasers and alcohol [17]. It also offers excellent thermo-forming properties with high stiffness and resilience [17]. For the experiments the substrate was cut to size from a sheet of PETG using an industrial scissor.

On the other hand, Macor is also preferred in BioMEMS applications due to its inertness, precision machinability and dimensional stability. It offers a number of properties including high resistivity to electric current and temperatures along with high dielectric strength, therefore it is used as insulator in surgical instruments [18]. Although other materials such as Nylon and plastics can be used as insulating materials but they are mostly unstable in areas of high cyclic stress, while Macor is resistive to vibration. For Macor's glass-ceramic substrate a linear precision saw (Model: IsoMet® 5000 by Buehler, IL, USA) was used to trim the square pallet to the desired size. Table 1 summarizes significant properties of both materials.

The formation of transmission spot lap joint using laser source usually requires the top substrate to be transparent so that the lower absorbent substrate undergoes localized melting at the interface. In our case both thermoplastic polyethylene terephthalate glycol (PETG) sheet (RS Components) and Macor glass-ceramic plate (Corning Inc.) have high absorptivity at a wavelength of 10.6 μm. However the melting temperature of PETG (78°C) is significantly lower than ceramic (1000°C) therefore ceramic substrate is placed on top of PETG. In this configuration, heat is transmitted from the ceramic to PETG which causes the latter to melt [see Fig. 1(a)]. Under the force of clamping a joint is formed at the interface upon re-solidification [6]. Under the force of clamping a joint is formed at the interface upon re-solidification and increased joint strength can be

Table 1.—Selected properties of Macor glass-ceramic [16] and thermoplastic PETG.

Property		Macor	PETG
Mechanical	Density (g/cm^3)	2.52	1.27
	Porosity	0%	—
	Hardness	250 (Knoop)	R115 (Rockwell)
	Compressive strength (MPa)	350	55
	Flexural strength (MPa)	104	79
Thermal	Maximum use temperature (no load)	1000°C	78
Electrical	Dielectric strength (MV/m)	39.4	16

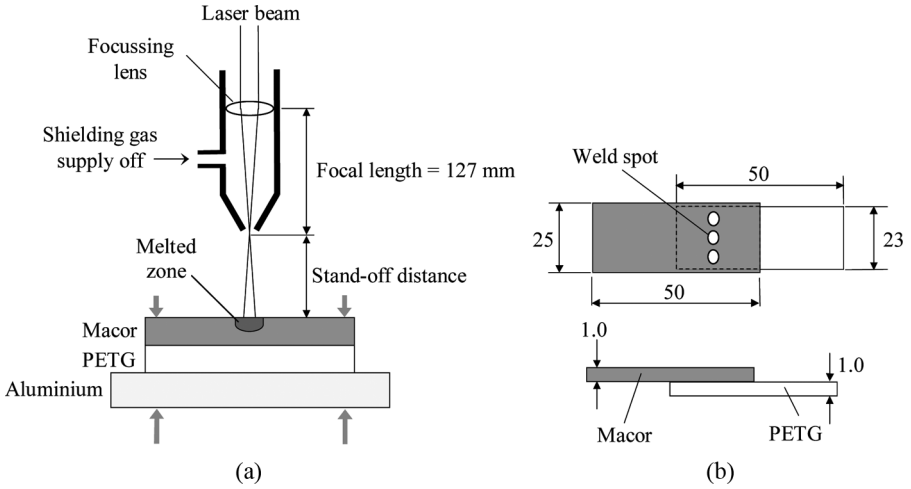

FIGURE 1.—(a) Schematic diagram of a laser spot welding. Laser beam is pointed on the Macor ceramic substrate for a predetermined exposure and some of the energy is subsequently transmitted to PETG polymer, and (b) schematic of samples (dimensions in mm).

achieved owing to the mechanical anchor effect upon re-solidification of plastic fluid inside the ceramic pores [6]. In the current configuration, Macor also acts as a clamping substrate thereby avoiding the need of brittle ZeSn as an optical window. It allows the transmission of heat to PETG and additionally minimizes degradation of PETG from chemical degradation, fusion and vaporization. At the bottom aluminum base plate is used due to its high reflectivity therefore minimizing heat loss to the surroundings. The minimum clamping pressure used for the all the experiments is kept at 8 kPa [9]. For experiments PETG substrate of dimensions 50 mm × 23 mm × 1 mm is used for spot welding with approximately similar sized Macor's glass-ceramic sample [see Fig. 1(b) for detailed drawing].

All experiments were carried out using a CO_2 laser (ZL1010 workstation and ZLX5 beam generation system). While using the mode structure TEM_{01} the CO_2 laser has a maximum power output of 500 W with an elliptical shape of the beam. The laser source can be operated in continuous wave (CW) as well as pulsed modes. In order to mount and maneuver the substrate assembly a purposely built working table was used with computer numeric control in all three axes. Table 2 summarizes the list of investigated process parameters and their levels. Three levels are selected for each process parameter so that the exact form of relationship can be deduced especially if nonlinearity is expected to exist. Initial assessment indicated linear relationship between tensile strength and all the factors. Given the higher cost of performing 3^3 (27) experiments, two levels for each factor were selected requiring a total of 2^3 (8) experiments. A summary of all parameters and their respective levels is presented in Table 2.

TABLE 2.—Notations and summary of all variables and experimental design levels used.

Notation	Parameter	Level 1	Level 2
f	Stand-off distance (mm)	23	31
E	Exposure (s)	2	4
n_s	Number of spots	1	3

It is important to mention here that the excessive dose of CO_2 pulsed laser may result in fracture cracking due to induced thermal stresses on ceramic substrate [19]. In addition it is known that at high laser power with short exposure time can lead to material removal of ceramic [20]. Therefore the current experiments were designed to use laser power at lower values with longer exposure durations. The preliminary run showed that the laser source in single pulses of longer durations can cause irradiation of the samples. Figure 1 shows the visuals of different durations of exposures (4, 5, and 6s) on the substrates. It is important to note that the number of spot joints, on a specific specimen, is dependent on the length of the sample substrate which in return is limited by the width of clamps on tensile machine. While the width of the spot welds depends on the stand-off distance of laser source and exposure duration.

In the present study, stand-off distance (f) is linearly related to the size of the laser beam (d) which incident on the ceramic substrate, where larger stand-off distance would give bigger beam spot size. The energy density (or power density) imparted on the workpiece is not only influenced by the duration of exposure but also affected by beam spot size as given by the following equation [6]:

$$\text{Energy density} = P/E/(\pi d^2/4) \quad (1)$$

where P is the laser power, E is the duration of exposure, and d is the diameter of the beam spot. Equation (1) shows that small beam spot size would give high energy density. It is noted that although high energy density is desirable for the present experiment, it could also result in unwanted crack in the ceramic and subsequently

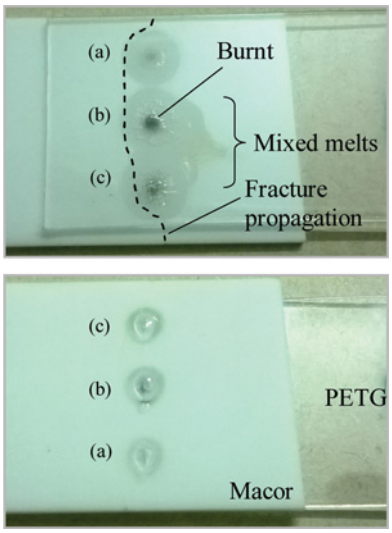

FIGURE 2.—Images taken after destructive test. Top image shows the weld qualities of three different spots taken at fixed laser power, stand-off distance of 27 mm and exposures of (a) 4, (b) 6, and (c) 5 s. Elliptical nature of the beam spot due to TEM_{01} mode structure is more recognizable on the ceramic side. Fracture propagation due to shear mode test is indicated with dotted line.

penetrating through the polymer with insufficient weld strength.

In order to avoid material removal or hole formation, the maximum duration of exposures has to be estimated. On the other hand excessive heat tends to increase spot diameter and occasional burns (as seen in Fig. 2). Therefore an optimal value of exposure duration has to be determined.

In addition estimation of minimum time delay between two consecutive pulses is also required. The delay time between two pulses influences the spot joint morphology. Figure 2 shows mixing of plastic melt from a spot with the melt zone of subsequent spot. The plastic melts of these two successive spots are likely to mix when insufficient cooling time is available. As the melted plastic expands volumetrically due to formation of bubbles, in case if two subsequent melted bubbles combine, the mixed molten material can move to the adjacent areas (as seen in Fig. 2). Experimental observation suggested that a minimum delay time of 3 s is required to avoid mixing of spot melt pools. Additionally spacing between two successive spot centers is kept at a minimum of 6.5 mm to avoid overlapping or heat conduction from the neighboring spot.

The parameters involving the eight experiments and the measured responses are listed in Table 3. We use a full-factorial experimental design to take into account all processing effects on weld qualities.

RESULTS AND DISCUSSION

The measurement of tensile strength of the weld leads to the destruction of the sample. Therefore the mean diameter of the weld spot was measured, prior to destructive testing, using the method illustrated in Fig. 3. The mean weld width is calculated as

$$\text{Mean weld width} = (\text{transverse diameter} + \text{conjugate diameter})/2$$

The conjugate and transverse diameters of the spot weld were measured using a digital microscope (resolution of 1 μm). The parameters were measured thrice and average value was obtained for each set of experiments. Variation in elliptical sizes between spots varies by about ±0.1 mm (minor axis or conjugate diameter) and ±0.16 mm (major axis or transverse diameter). Overall, the spot diameters have variation that is less than 2%.

The second test involved a tensile test performed on a universal tensile test machine (Instron 3369) of 50 kN capacity with load accuracy of 0.5%. For all experiments a fixed loading rate of 0.5 mm/min was used. The maximum tensile load at which the welded joint fails

TABLE 3.—Experimental layout and multi-performance results.

Experiment no.	Welding parameters			Mean weld diameter (mm)	Weld tensile strength (N)	Mean weld tensile strength (N)
	f (mm)	E (s)	n_s			
1	23	2	1	3.975	61.8	61.8
2	23	4	1	6.233	169.8	169.8
3	23	2	3	5.175	163.6	54.5
4	23	4	3	6.192	236.0	78.7
5	31	2	1	4.055	46.4	46.4
6	31	4	1	5.916	168.7	168.7
7	31	2	3	5.314	159.5	53.2
8	31	4	3	6.120	251.1	83.7

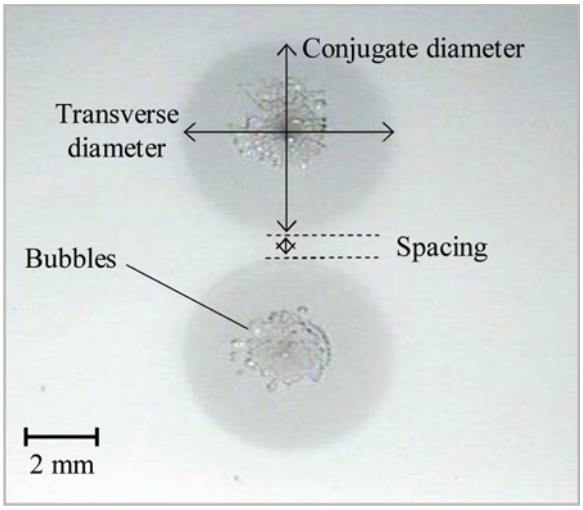

FIGURE 3.—Experiment no. 9 (Sample 5) PETG on top of ceramic substrate—before destructive tensile test. Variation in elliptical sizes between spots varies by about ±0.1 mm (minor axis or conjugate diameter) and ±0.16 mm (major axis or transverse diameter). Overall, the spot diameters has variation that is less than 2%.

was taken as its tensile strength. As test leads to failure of the sample only one reading is obtainable. For the calculation of mean tensile strength, the measured tensile strength is divided by the number of spots. All measurements are reported in Table 3.

It is instructive to comment on peel-off failure mode tests. The tests were performed by holding the ceramic substrate along both edges, and pulling the polymer substrate perpendicular to the surface. For all experiments a fixed loading rate of 0.5 mm/min was used using the same Instron tensile test machine. Because the thickness of the ceramic is physically thin (1 mm), majority of the ceramic substrates would crack due to its brittleness when clamping force is applied to avoid slippage. In addition, it was laboriously difficult to keep the sample perpendicular to the pulling direction throughout the experiment without damaging the ceramic. Since majority of the samples did not successful during peel test, the authors cannot quantitatively determine the reliable peel-off forces. Nevertheless, it can be said that in general the force required for peel test is considerably less than that of shear test.

When laser is incident on the Macor substrate (glass-ceramic), the heat generated modifies its microstructure. At this point, the heat causes some part of the glass-ceramic to melt again and eventually re-solidify but the process now occurs in uncontrolled conditions compared to the original production conditions [21]. The controlled process parameters result in unstructured crystal growth while glass re-crystallization. This results in bubbles formation due to internally nucleated fluormica crystals. Moreover due to the temperature dependent nature of nucleation rate, the formation and morphology of bubbles is also expected to be temperature dependent [22]. During the process hissing can be observed suggesting the formation of bubbles with varying sizes and quantity, seen on the ceramic substrate (see Fig. 9 in Ref. [9]). However only top surface of the ceramic underwent microstructure modification while the bottom surface which firmly clamped to the polymer was observed remained in its original state. On the other hand, the transmitted heat from the ceramic causes the polymer to melt due to its low melting point (about 78°C). The interaction also results in the formation of bubbles of varying sizes and quantity which depend on the heat transmitted. As seen in Fig. 3, these bubbles predominantly exist on the central region of the spot.

Figure 4 shows different fracture propagation of some samples having different number of spots after the tensile test. Visual inspection showed no elongation observed with respect to PETG. However, as seen in Fig. 4, PETG remains firmly attached to the ceramic in all the cases while the failure occurred in the ceramic substrate. It is important to mention that the observation does not suggest that the weld strength is stronger than the parent ceramic substrate. Using tensile test, the strength of parent ceramic was measured as 480 N [9]. While joining PETG with ceramic, Tamrin et al. [9] pointed out that the failure of all test samples concerning lap joint of ceramic-PETG occurred in this

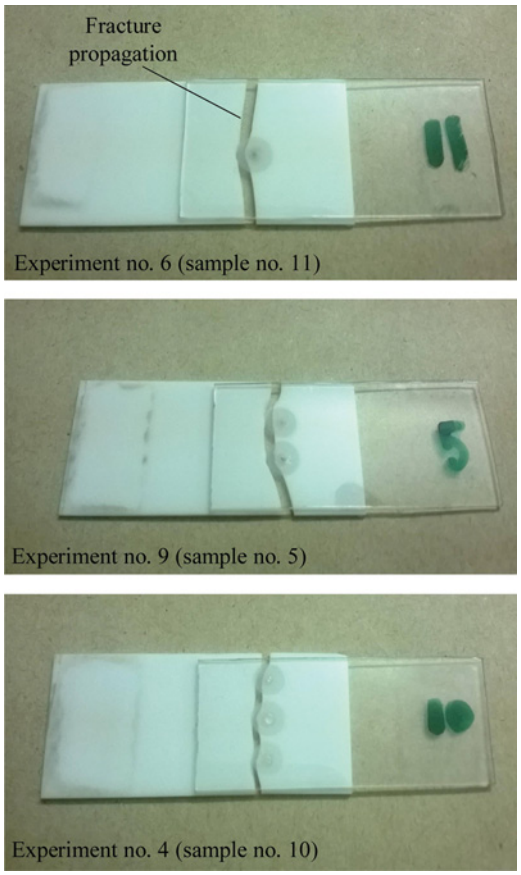

FIGURE 4.—Fracture propagation of different samples having different number of spots.

region due to the formation of re-crystallized glass. From this, it can be inferred that fracture could be originated at the weld spot as it is likely to have the weakest strength which then promotes fracture propagation throughout the rest of ceramic substrate. The fracture also appears to be propagating around the weld spot suggesting that the center spot having the strongest welded joint and it gets weaker further away from the center.

In addition, the variation of mean tensile strength is also plotted against the mean spot diameter (see Fig. 5). It can be observed from the figure that that the mean weld tensile strength shows no direct dependence on the means weld diameter.

Figure 6 shows the effect of laser exposure (s) on the tensile strength of the spot joints. Figure 6 also highlights the number of spots and standoff distance for each data point. It can be observed that the tensile strength increases with the laser exposure. In addition, the effect of number of spots also results in the increase of tensile strength of the joint. For instance in case of 2.0s exposure duration, an increase of 100N in the tensile strength is observed with the increase of number of spots from 1 to 3, suggesting a 50N increase of strength per additional spot. A similar trend can be seen for the case of 4.0s exposure duration. While the effect of stand-off

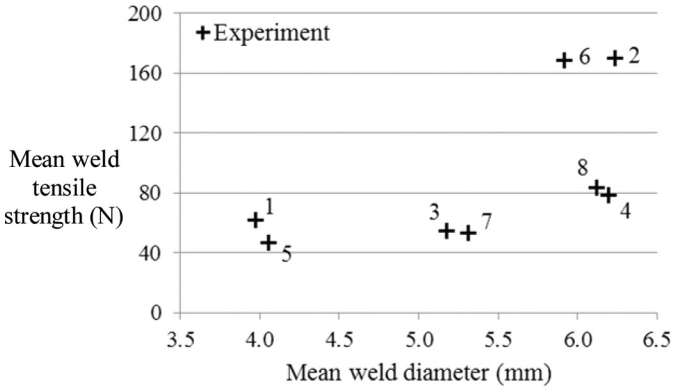

FIGURE 5.—Variation of the mean tensile strength with mean weld width. Each marker is labeled with its experiment number as shown in Table 3.

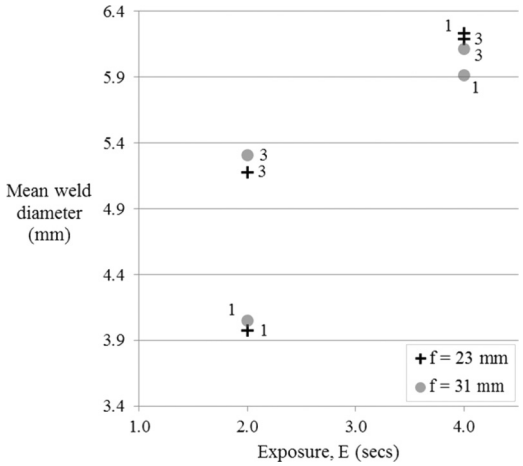

FIGURE 7.—Variation of the mean weld diameter with laser exposure at different stand-off distance and number of spots. The number of spots is shown next to the marker.

distance is somewhat inconclusive as no direct relation can be obtained for tensile strength variation with stand-off distance. Instead the effect of stand-off distance is quite marginal compared to the effect of exposure duration and number of spots on the tensile strength of the specimen. At low laser power the effect of stand-off distance is expected to have lesser influence as observed in Fig. 6.

Figure 7 includes the effect of all three parameters (exposure, stand-off distance, and number of spots) on the mean weld diameter. As observed in the case of weld tensile strength, the effect of stand-off distance is quite insignificant on the mean weld diameter (see Fig. 7). At the low laser power no clear trend can be deduced for the stand-off distance on the weld diameter, however [23] showed that the weld width is dependent on stand-off distance also. On the other hand increase in laser exposure duration causes an increase of mean weld diameter. The number of spots seems to affect the mean weld diameter at lower exposure duration mainly. While at 4 s exposure duration the mean weld widths remains

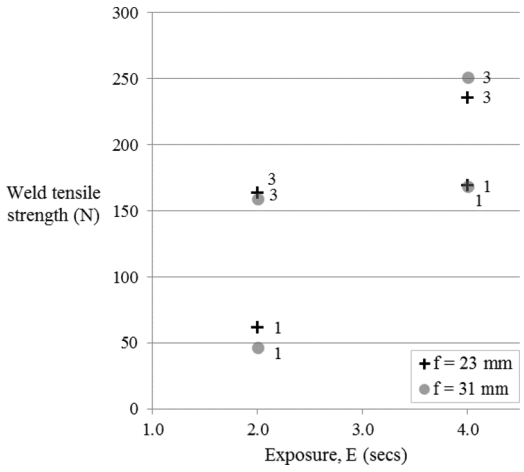

FIGURE 6.—Variation of the tensile strength with laser exposure at different stand-off distance and number of spots. The number of spots is shown next to the marker.

approximately same irrespective of number of spots. At lower exposure duration of 2 s, a larger variation is observed primarily due to variation in the major and minor diameters of the spots. At lower operating powers CO_2 laser is quite unstable and may lead to inconsistent power prevalence. This may cause a strong variation of mean spot diameter at lower exposure durations.

In such circumstances it is difficult to assort the optimal processing parameters for repeatable and consistent results. Therefore based on the experimental data, a more detailed analysis can be performed to evaluate optimal configuration. A number of studies [15] use multi-objective optimization on the basis of ratio analysis (MOORA) to find optimal configuration of processing parameter. The same analysis is used to estimate the configuration that suits the spot welding process for the case considered. As the name indicates, multi-objective optimization procedure carries out simultaneous optimization of multiple attributes in a given set of constrains. Introduced by Brauers and Zavadskas [24], MOORA has been used for various problems especially in optimization of manufacturing processes [25]. It is a matrix based method and starts with the formation of a decision matrix [Eq. (3)]. The decision matrix comprises of the measured performances of different variables for various objectives.

$$X = \begin{bmatrix} x_{11} & x_{12} & \dots & \dots & \dots & \dots & x_{1n} \\ x_{21} & x_{22} & \dots & \dots & \dots & \dots & x_{2n} \\ \dots & \dots & \dots & \dots & \dots & \dots & \dots \\ \dots & \dots & \dots & \dots & \dots & \dots & \dots \\ x_{m1} & x_{m2} & \dots & \dots & \dots & \dots & x_{mn} \end{bmatrix} \quad (3)$$

Each values of measured performance x_{mn} are noted for all alternatives/variables with attributes/objectives. Where m represents the total number of alternatives, while n represents the total number of attributes. In the second step a ratio is calculated of all the performance of

alternatives for an attribute. This ratio, calculated using Eq. (4), represents all alternatives concerning a specific attribute.

$$\overset{a}{x}_{ij} = \frac{x_{ij}}{\sum_{i=1}^{m} x_{ij}^2} \quad (j = 1, 2, \ldots, n) \tag{4}$$

where the normalized performance parameter x_{ij} represents ith alternative on jth attribute ranging from [0, 1]. In order to optimize the configuration, these parameters are either added for maximum beneficial attributes or subtracted for minimum non-beneficial attributes, as shown in Eq. (5).

$$\bar{y}_i = \sum_{j=1}^{g} w_j \cdot \overset{a}{x}_{ij} - \sum_{j=g+1}^{n} w_j \cdot \overset{a}{x}_{ij} \quad (j = 1, 2, \ldots, n) \tag{5}$$

For maximization g is the total number of attributes, while for minimization the number of attributions is presented by $(n - g)$. Normalized value of $\bar{y}_i$ represents the assessment for ith substitute compared to all attributes. In case if an attribute is of more importance than others, a weighing parameter w_j (for jth attribute) can also be included. The value of $\bar{y}_i$ can be positive (maxima-beneficial attributes) or negative value (minima-negative attribute), while the ordinal ranking indicates the final preferences.

Table 4 shows the normalized decision-making matrix and results of MOORA. Because we cannot determine the exact relationship between weld tensile strength and weld diameter (see Fig. 5), each quality is assigned equal weight of $w_j = 1$. This means that each quality is equally important. The respective ranking of each experimental set is also shown in Fig. 8 using MOORA. It can be observed that the experiment number 8 has the highest normalized multi-criteria value with most number of spots and the longest duration of laser exposure. While the experiment number 4 is ranked second with same credentials of number of spots and exposure. The only difference between the rank 1 and 2 is the stand-off distance. Interestingly the effect of stand-off distance was not dominant in previous sections. Quite clearly here the stand-off distance is providing the rank difference between experiment number 8 and 4. Experiment number 8 with larger stand-off distance is ranked 1. On the other hand the experiment number 5 has the lowest value with least number of spots and shortest exposure. Interestingly experiment number 1 is ranked 7 with similar attributes of experiment number 5. The only difference between the two is that the stand-off distance of rank 7 is less than rank 8. Therefore a reverse trend is observed for assignment of lowest ranks.

TABLE 4.—Normalized decision-making matrix and results of multi-objective analysis.

Exp.	Mean weld diameter (mm)	Weld tensile strength (N)	Normalization: Mean weld diameter	Normalization: Weld tensile strength	$\bar{y}$	MOORA rank
1	3.975	61.8	0.2583	0.1277	0.3860	7
2	6.233	169.8	0.4050	0.3509	0.7559	3
3	5.175	163.6	0.3363	0.3380	0.6743	6
4	6.192	236.0	0.4023	0.4876	0.8900	2
5	4.055	46.4	0.2635	0.0959	0.3594	8
6	5.916	168.7	0.3844	0.3486	0.7330	4
7	5.314	159.5	0.3453	0.3296	0.6749	5
8	6.120	251.1	0.3977	0.5188	0.9165	1
$\sum_{j=1}^{8} x_{ij}^2$	236.907	234,216.4				
$\sum_{j=1}^{8} x_{ij}^2$	15.392	484.0				

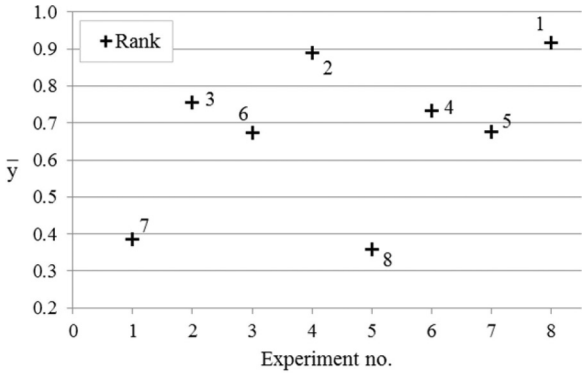

FIGURE 8.—Graph of MOORA results.

Quite clearly MOORA result shows that the influence of stand-off distance can be deterministic while estimating the overall optimal performance parameters. For the other two parameters (exposure and number of spots) the results are confirmative of the analysis carried out in previous section. MOORA rankings reveal that the differentiating parameter for the best and worst configuration for the reported experiments is the stand-off distance. However the exact influence of stand-off distance at lower operating powers cannot be found. For such analysis a detailed parametric study on the mechanics of the joint due to varying stand-off distance is recommended.

CONCLUSIONS

The effect of different laser processing parameters on the strength of spot welding and spot diameter is studied here. Following important conclusions can be drawn for the range of parameters considered. Increase in tensile strength is observed with the increase of laser exposure and number of spots. With each additional spot weld a substantial increase of joint strength is seen. While extended laser exposure causes an increase of spot weld mean diameter. Although the effect of stand-off distance is not substantial, still an optimal configuration obtained using MOORA technique is observed to have a larger stand-off distance. However at low laser powers the effect of stand-off distance on the joint strength requires extensive study.

Funding

The authors are grateful to the Ministry of Higher Education Malaysia for the FRGS grant (FP039-2013B) allocated to the project.

References

1. Steen, W.M.; Mazumder, J.; Watkins, K.G. *Laser Material Processing*; Springer: London, UK, 2003.
2. Wahba, M.; Kawahito, Y.; Katayama, S. Laser direct joining of AZ91D thixomolded Mg alloy and amorphous polyethylene terephthalate. *Journal of Materials Processing Technology* **2011**, *211* (6), 1166–1174.
3. Katayama, S.; Kawahito, Y. Laser direct joining of metal and plastic. *Scripta Materialia* **2008**, *59* (12), 1247–1250.
4. Kawahito, Y.; Nishimoto, K.; Katayama, S. LAMP joining between ceramic and plastic. *Physics Procedia* **2011**, *12*, 174–178.
5. Lubna, N.; Newaz, G. Analysis of titanium-coated glass and imidex (PI) laser bonded samples. *Journal of Materials Engineering and Performance* **2012**, *21* (2), 266–270.
6. Tamrin, K.F.; Nukman, Y.; Zakariyah, S.S. Laser lap joining of dissimilar materials—A review of factors affecting joint strength. *Materials and Manufacturing Processes* **2013**, *28* (8), 857–871.
7. Ruedas-Rama, M.J.; Walters, J.D.; Orte, A.; Hall, E.A. Fluorescent nanoparticles for intracellular sensing: A review. *Analytica Chimica Acta* **2012**, *751*, 1–23.
8. Okabe, K.; Inada, N.; Gota, C.; Harada, Y.; Funatsu, T.; Uchiyama, S. Intracellular temperature mapping with a fluorescent polymeric thermometer and fluorescence lifetime imaging microscopy. *Nature Communications* **2012**, *3*, 705.
9. Tamrin, K.F.; Nukman, Y.; Sheikh, N.A.; Harizam, M.Z. Determination of optimum parameters using grey relational analysis for multi-performance characteristics in CO_2 laser joining of dissimilar materials. *Optics and Lasers in Engineering* **2014**, *57*, 40–47.
10. Dubey, A.K.; Yadava, V. Laser beam machining—A review. *International Journal of Machine Tools and Manufacture* **2008**, *48* (6), 609–628.
11. Meijer, J. Laser beam machining (LBM), state of the art and new opportunities. *Journal of Materials Processing Technology* **2004**, *149* (1), 2–17.
12. Yusof, F.; Miyashita, Y.; Hua, W.; Mutoh, Y.; Otsuka, Y. YAG laser spot welding of PET and metallic materials. *Journal of Laser Micro Nanoengineering* **2011**, *6* (1), 69–74.
13. Holtkamp, J.; Roesner, A.; Gillner, A. Advances in hybrid laser joining. *International Journal of Advanced Manufacturing Technology* **2010**, *47* (9–12), 923–930.
14. Tamrin, K.F.; Nukman, Y.; Choudhury, I.A.; Shirley, S. Multiple-objective optimization in laser cutting of different thermoplastics. *Optics and Lasers in Engineering* **2014**, *67*, 57–65.
15. Gadakh, V.; Shinde, V.; Khemnar, N. Optimization of welding process parameters using MOORA method. *The International Journal of Advanced Manufacturing Technology* **2013**, *69* (9–12), 2031–2039.
16. Höland, W.; Beall, G.H. *Glass Ceramic Technology*; Wiley: Hoboken, NJ, 2012.
17. Becker, H.; Locascio, L.E. Polymer microfluidic devices. *Talanta* **2002**, *56* (2), 267–287.
18. Wuchinich, D.G. Endoscopic Ultrasonic Rotary Electro-Cauterizing Aspirator. Google Patents, US5176677A, 1993.
19. Lei, H.; Lijun, L. A study of laser cutting engineering ceramics. *Optics & Laser Technology* **1999**, *31* (8), 531–538.
20. Samant, A.N.; Dahotre, N.B. Laser machining of structural ceramics—A review. *Journal of the European Ceramic Society* **2009**, *29* (6), 969–993.
21. Beall, G.H.; Chyung, C.-K.; Watkins, H.J. Mica Glass-Ceramics. US Patent 3,801,295, 1974.
22. Höland, W.; Rheinberger, V.; Schweiger, M. Control of nucleation in glass ceramics. *Philosophical Transactions of the Royal Society of London. Series A: Mathematical, Physical and Engineering Sciences* **2003**, *361* (1804), 575–589.
23. Wang, X.; Song, X.H.; Jiang, M.F.; Li, P.; Hu, Y.; Wang, K.; Liu, H.X. Modeling and optimization of laser transmission joining process between PET and 316 L stainless steel using response surface methodology. *Optics and Laser Technology* **2012**, *44* (3), 656–663.
24. Brauers, W.; Zavadskas, E.K. The MOORA method and its application to privatization in a transition economy. *Control and Cybernetics* **2006**, *35*, 445–469.
25. Chakraborty, S. Applications of the MOORA method for decision making in manufacturing environment. *The International Journal of Advanced Manufacturing Technology* **2011**, *54* (9–12), 1155–1166.